Interference cancellation for radio astronomical images

Ronny Levanda and *Amir Leshem*
School of Engineering Bar Ilan University, 52900 Ramat Gan, Israel.
{ronny.levanda, leshem.amir}@gmail.com

Abstract

We propose a new algorithm, for parameter estimation that is applicable to imaging using moving and synthetic aperture arrays. The new method results in higher resolution and more accurate estimation than commonly used methods when strong interfering sources are present inside and outside the field of view (terrestrial interference, confusing sources).

1 Introduction

When multiple antennas or other sensors are used to estimate incoming signals, it is best to treat them all as a single array and apply one of the known array processing algorithms to do the estimation. In various situations, however, this is not practical or even impossible.

In radio-astronomy (see [1,2] for a good overview), the antenna array moves with the rotation of the Earth. Correlations between the antenna can be obtained for a given time, but not between different points in time. Denote by $\mathbf{R}_k$ the measured correlation matrix (visibility) of the array at time t_k; The standard approach to estimate the power per incident angle (also known as the *dirty image*), $\hat{I}(l,m)$ is

$$\hat{I}(l,m) = \frac{1}{K}\sum_{k=1}^{K} \mathbf{w}_k^H(l,m)\mathbf{R}_k\mathbf{w}_k(l,m), \tag{1}$$

where $\mathbf{w}_k(l,m)$ is the beamformer weight vector calculated according to the beamformer used and (l,m) are the cosines of the incident angle. The reader is referred to [3-5] for an overview of the matrix based approach and equivalency between Equation (1) and the visibility Fourier transform. The reader is also referred to [1-3,6,7] for imaging techniques.

In this paper we demonstrate the performance of a novel method (first introduced at [10]) over two dimensional images. We use two beamformer weight vectors, the classic (i.e., Bartlett) beamformer which is equivalent to the standard approach and the MVDR (minimum-variance-distortionless-response) beamformer desinged to obtain high SNR for images with interferance (see [8,9]). The classic beamformer weight vector is given by $\mathbf{w}_k(l,m) = \frac{1}{P}\mathbf{a}_k(l,m)$, where $\mathbf{a}_k(l,m)$ is the array steering vector at the k'th measurement epoch defined by $\mathbf{a}_k(l,m) \equiv \left(e^{\frac{-2\pi j}{\lambda}(x_1^k l + y_1^k m)}, \ldots, e^{\frac{-2\pi j}{\lambda}(x_P^k l + y_P^k m)}\right)^T$. (x_i^k, y_i^k) is the location of antenna i at the k'th measurement time, (l,m) are the direction cosines, λ is the wavelength and P is the number of antennas used. The MVDR beamformer, weight vector is given by $\mathbf{w}_{\mathtt{mvdr}}^H = \frac{\mathbf{a}^H\mathbf{R}^{-1}}{\mathbf{a}^H\mathbf{R}^{-1}\mathbf{a}}$.

2 Adaptive Selective Sidelobe Canceller Beamforming

In this section we present a novel image formation technique. We begin with a simple example that demonstrates the main idea behind the adaptive-selective-sidelobe-canceller (ASSC) algorithm; for a specific observation direction, the received interference through the sidelobes varies strongly as the array rotates.

For simplicity, consider an East-West linear array with 20 antennas, $\lambda/2$ spaced. Observation is done every 6 minutes for a 12-hour period. The measured correlation matrix at the k'th epoch is $\mathbf{R}_k$. For a specific direction (l,m), the output of the k'th beamformer, $\hat{I}_k = \mathbf{w}_k^H\mathbf{R}_k\mathbf{w}_k$, is composed of the signal-of-interest

978-1-4244-6051-9/11/$26.00 ©2011 IEEE

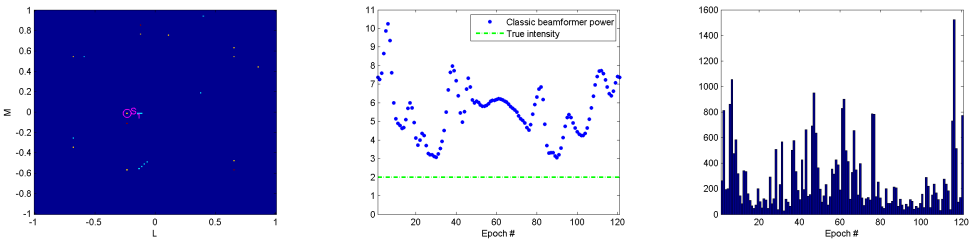

a b c

Figure 1: a - Original image. b - output power for all time epochs of the classic beamformer for S_1. c - Number of pixels ((l, m) directions), a specific measurement (time epoch) estimated the minimal power (i.e., underwent the smallest interference)

(SOI) contribution, interfering sources and the noise contribution. The contribution of the interfering sources is determined by their location (and strength) relative to the array sidelobes. Consider a scenario with a few clusters of sources (see Figure (1a)). Figure (1b) shows the output power of the k'th classic beamformer for a direction of a point source S_1 (marked at Figure (1a)). From all available time epochs, only a few epochs yield an estimation close to the true point source intensity. The intensity estimation of most epochs is biased due to the interference (received through their sidelobes). The time epoch with the *minimal power for a specific direction* yields the best estimator. Averaging the output power for all epochs will result in a biased and inaccurate estimator.

Note that although the number of reliable estimates per direction is small, the total number of correlation matrices for the entire FOV is much larger (it depends on the interference location and the array geometry). Histograms of the number of directions (pixels) for which a specific correlation matrix estimated the minimal power (i.e., underwent the smallest interference) is shown in Figure (1c). For the classic beamformer, out of the 181×181 pixels in the image, most time epochs (more than 90%) performed best (i.e.,had minimal interference) for at least 661 pixels. Over 65% of the time epochs benefited from minimal interference for 90% of the pixels in the image.

This example demonstrates that the received array power of a specific (l, m) observation direction, varies significantly with the array orientation due to interfering sources. Some of the array orientations yield a reliable intensity estimation, whereas others yield a biased intensity estimation (aggravated by the interfering signals).

2.1 The ASSC algorithm

For a given set of R_k correlation matrices, $k = 1 \dots K$, measured at K time epochs:

- Calculate the array output power (i.e., dirty image) *for each epoch separately* according to the desired beamformer weight vector.
- Determine the ASSC parameters $\tilde{k}$ and μ_k where $\tilde{k}$ is the number of best epochs to consider for each (l, m) and μ_k are their weights. These parameters are best determined using the measured data by plotting a histogram of the calculated $\hat{I}_k(l, m)$ for a specific (l, m). $\tilde{k}$ is determined so no epoch that suffers from significant sidelobes (i.e., has significantly larger power than the minimal power) will be selected. Typically $\tilde{k} < 5\%$ depending on the array geometry and the interference strength and location. As a rule of thumb, the stronger the interference, the smaller the $\tilde{k}$.As for μ_k, is should be chosen such that $\mu_{k+1} \leq \mu_k$.
- For each (l, m) (each pixel in the image) find the best (i.e., smallest) $\tilde{k}$ values among all measurements.

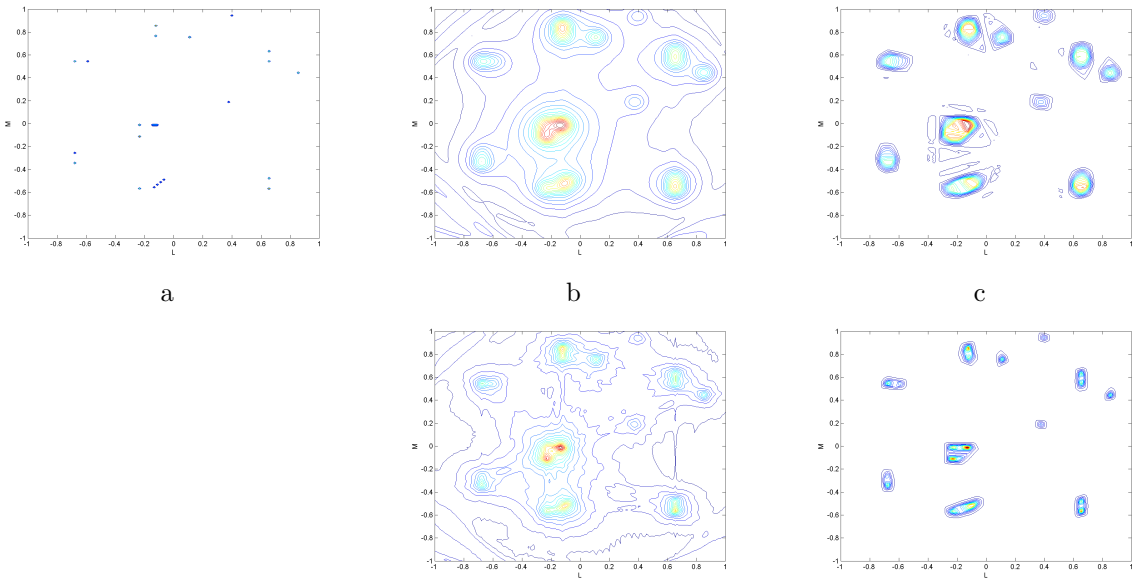

Figure 2: Example of dirty images for a few clusters of sources. a - Original image. b - Classic beamformer image. c - ASSC classic beamformer image. d - MVDR beamformer image. e - ASSC MVDR beamformer image. All images are plotted using the same number of contours.

- Calculate the ASSC power (dirty image) according to a weighted average of the $\tilde{k}$ smallest estimations.

3 Simulation results

3.1 In FOV interference

This section reports on ASSC algorithm performance compared to existing techniques (classic and MVDR) for the example discussed in (2). The ASSC parameters are $\tilde{k} = 3$ and $\mu_k = 1$. Figure (2a) shows the original image that contains a few clusters of sources. Using the classic beamformer (Figure (2b)), the resulting image (classic dirty image) has wide peaks around each cluster of sources, and the noise is high. The ASSC classic beamformer yield a much quieter image (Figure (2c)). The MVDR (Figure (2d)) beamformer image has higher spatial resolution than the classic beamformer (as expected). The ASSC MVDR beamformer (Figure (2e)) has higher resolution than the MVDR and has the advantage of a quiet image.

3.2 Strong out-of-FOV interference

This section presents examples of a very strong interference 10^6 times the power of the desired sources. Using an East-West array with 20 antennas logarithmically spaced $0 - 200\lambda$. Measurement was done every minute for a 12-hour period. The ASSC parameters used were $\tilde{k} = 5$ (out of the 719 available orientations) and $\mu_k = \frac{1}{\tilde{k}}$. Figure (3a) shows the original observed image with 6 point sources. The strong interference is not seen in the image (since the interferer is out of the field of view). The output of the classic and MVDR beamformer (dirty images) are shown in Figures (3b) and (3c) respectively. The entire image is smeared with the strong interferer sidelobes. The point sources are not seen. The output of the ASSC MVDR beamformer is shown in Figure (3d). The point sources are seen clearly and the strong interferer sidelobes do not appear

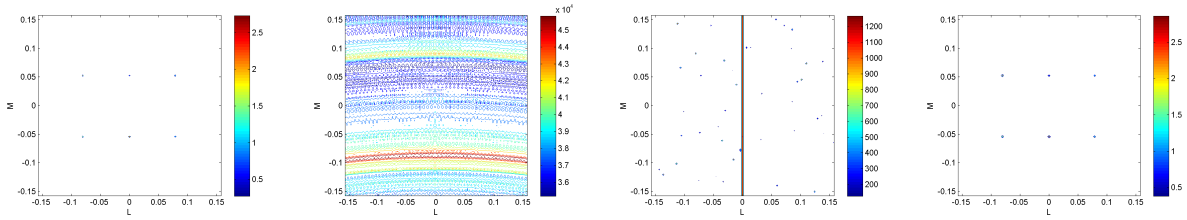

a b c d

Figure 3: Dirty images of 6 point sources and a strong interfering source outside of the field of view. a - Original image. b - classic beamformer image. c - MVDR beamformer image. d - ASSC MVDR beamformer image.

in the image at all since only correlation matrices that are affected negligibly from the sidelobes are selected.

4 Summary

In this paper we introduced the ASSC beamformer, a method to combine rotating/many array measurements for interference suppression. The performance of the ASSC (classic and MVDR) were demonstrated and compared to the classic and MVDR beamformer. For interference dominant cases, the ASSC beamformer obtains images with higher spatial resolution and interference cancelation than either the classic or the MVDR beamformer.

5 Acknowledgments

This research was supported by ISF grant 1240/09: Signal processing and imaging for large radio telescopes.

6 References

1. G.B. Taylor and C.L. Carilli and R.A. Perley. Synthesis Imaging in Radio-Astronomy. Astronomical Society of the Pacific 1999.

2. A.R. Thompson and J.M. Moran and G.W. Swenson. Interferometry and Synthesis in Radio astronomy, John Wiley and Sons 1986.

3. R. Levanda and A. Leshem, Synthetic aperture radio telescopes, IEEE Signal Processing Magazine Jan 2010, vol 27, pages 14-29.

4. C. Ben-David and A. Leshem. Parametric High Resolution Techniques for Radio Astronomical Imaging. IEEE Journal of Selected Topics in Signal Processing Oct 2008, vol 2, pages 670-684.

5. A.J. van der Veen and A. Leshem and A.J. Boonstra, Array signal processing in radio-astronomy,Experimental Astronomy June 2004, vol , pages 231-249.

6. T.J. Cornwelltitl. Multiscale CLEAN Deconvolution of Radio Synthesis Images. IEEE Journal of Selected Topics in Signal Processing Oct 2008, vol 2, number 5, pages 793-801.

7. U. Rau and S. Bhatnagar and M.A. Voronkov and T.J. Cornwell. Advances in Calibration and Imaging Techniques in Radio Interferometry. Proceeding of the IEEE Aug 2009, vol 97, pages 1472-1481.

8. J. Capon, High resolution frequency-wavenumber spectrum analysis, Proceedings of the IEEE, pages 14081418, 1969.

9. H. V. Trees, Optimum array processing. J. Wiley, 2002.

10. R. Levanda and A. Leshem. IEEE 26-th Convention of Electrical and Electronics Engineers in Israel 2010.